ACS OMEGA

Article

Cite This: ACS Omega 2018, 3, 8709−8717

http://pubs.acs.org/journal/acsodf

Enrichment of Surface-Active Compounds in Bursting Bubble Aerosols

Konstantin Chingin, Runhan Yan, Dacai Zhong, and Huanwen Chen*

Jiangxi Key Laboratory for Mass Spectrometry and Instrumentation, East China University of Technology, Nanchang 330013, China

ABSTRACT: The pronounced enrichment of surface-active compounds in the aerosols produced by bubble bursting plays a central role in the chemical transfer from the ocean into the atmosphere and has an important impact on the global Earth's climate. However, the mechanism of chemical enrichment in bursting bubble aerosols remains poorly understood and controversial due to the high complexity and diversity of experimental behaviors. Contrary to the common belief, here we show that the major share of surfactants in the jet droplets produced by individually bursting bubbles at a calm solution surface is released directly from the bubble surface rather than from the solution surface or subsurface microlayer. We reveal that surfactants are accumulated at the surface of a rising bubble in solution following three successive stages with strongly distinct adsorption profiles: linear kinetic, mixed kinetic, and equilibrium. The magnitude of surfactant enrichment in the aerosol is directly determined by which adsorption mode is in control by the moment of the bubble bursting at solution surface. Our mechanistic description explains the diversity of experimental observations regarding the surfactant enrichment in aerosol droplets and lays the ground for understanding the more complex behaviors associated with collective effects at the solution surface (e.g., breaking waves).

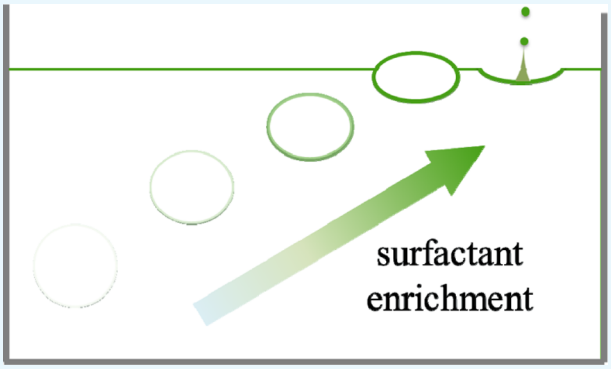

INTRODUCTION

Bursting of gas bubbles at a liquid−air interface is a common phenomenon in many natural and industrial processes,[1−6] the most common examples being the formation of sea spray aerosol[7−12] and the effervescence of sparkling beverages.[13−18] The mechanism of bursting bubble aerosol formation has been extensively studied for several decades, both from the physical[17−22] and chemical[23−27] points of view. One of the most interesting aspects of the bubble bursting process is the substantial enrichment of surface-active organic matter in the bursting bubble aerosol relative to the bulk solution.[26−30] Earlier studies revealed that soluble organic carbon in sea spray aerosols is enriched by, on average, several hundred times relative to the bulk sea water,[27] and this phenomenon has an important impact on the global Earth's climate.[10,28,29] It has been also demonstrated that the enriched content of surface-active compounds in fizzy aerosols is largely responsible for the characteristic organoleptic properties of sparkling beverages.[13,17] Recently, bubble bursting has also been demonstrated as a potentially useful approach for the analytical preconcentration of organic solutes.[31,32]

Unfortunately, the comprehensive investigation of bubble bursting process and associated enrichment of surface active compounds is greatly complicated due to the broad diversity and high transience of processes at the water−air interface.[33,34] These processes may include bubble coalescence,[35] foaming,[36] nonequilibrium mixing at the air−liquid interface,[30] intermolecular interactions,[30,32,37] turbulence effects,[21] nucleation,[38] as well as different modes of bubble bursting, depending on both the size of bubbles[22,39,40] and the surface tension of the solution.[17,41] These processes not only increase the mechanistic complexity but also significantly affect the reproducibility of experimental behaviors.[34] As a result, the chemical transfer by bubble bursting remains poorly explored and controversial. Thus, there is yet no agreement whether surface-active organic compounds are mainly released into the atmosphere directly from the bubble surface,[24,42,43] solution surface, or the subsurface microlayer.[33,44−46] Another poorly studied aspect is the dynamics of surfactant accumulation via nonequilibrium molecular adsorption on rising bubbles in solution and the establishment of molecular equilibrium at the bubble surface. Currently, it remains largely unknown whether the chemical enrichment in bursting bubbles can be reliably predicted using adsorption models developed for stationary liquid−air interfaces.[47,48] Apparently, surfactant enrichment in bursting bubble aerosols is a highly complex behavior, and many more mechanistic studies under simplified and well-controlled settings are required for the better understanding of underlying mechanisms.[34]

This study contributes new data on the adsorption process of organic species at the surface of rising bubbles in the water as well as on the process of the bubble bursting.

Received: May 30, 2018
Accepted: June 15, 2018
Published: August 7, 2018

DOI: 10.1021/acsomega.8b01157
ACS Omega 2018, 3, 8709−8717

Concentrations of rhodamine dyes in the aerosol phase are related to the bubble traveling path in solution as well as to rhodamine concentration in solution. Three stages of interaction between the bubbles and aqueous solution are identified: linear kinetic adsorption, mixed kinetic adsorption, and equilibrium adsorption. Comprehensive mechanistic interpretation of surfactant enrichment in bursting bubble aerosol is provided.

EXPERIMENTAL SECTION

The concentration enrichment in bursting bubble aerosol, relative to the bulk solution ($E = C_{aer}/C_{bulk}$), was studied for three individual room-temperature aqueous solutions of rhodamine dyes, rhodamine 101 (R101), rhodamine B (RB), and rhodamine 6G (R6G). These three rhodamine dyes were selected for their environmental relevance as common contaminants,[49,50] high and well-studied surface activity,[51] as well as for the high sensitivity of quantitative detection. This allowed the determination of E-values in a broad range of C_{bulk} (10^{-8}−10^{-4} M). Nitrogen bubbles in individual water solutions of RB (99.75% purity; Xilong Chemical company, Guangzhou), R101 (99.9% purity; Sigma-Aldrich, Shanghai), and R6G (99.9% purity; Macklin Biochemical company, Shanghai) were generated at ambient conditions by feeding neutral nitrogen gas through an air diffuser (0.2−5 μm pore size; diameter, 23 mm; height, 5 mm; custom manufactured in the glass facility of Nanchang University) at the bottom of solution (diameter, 10 cm; height, 1−100 cm). Inert nitrogen gas was chosen for the simplicity of mechanistic consideration. The large diameter of solution vessel (10 cm), relative to the diameter of the diffuser (2.3 cm), was chosen to prevent the collisions of rising bubbles with the walls of the vessel. To minimize the role of interfacial processes at the solution surface associated with bubble foaming, coalescence, and other collective effects, as well as to reduce the bubble coalescence and turbulence, the bubbling flow rate was brought to a minimal possible level, at which stable bursting process could still be achieved (2 mL/min). The average diameter of rising bubbles under those conditions was ca. 0.5 mm and was not visibly changed with bubble path. The speed of rising bubbles was ca. 20 cm/s and was not measurably altered during the bubble rise in solution. The bubble path was adjusted from ca. 1 to 100 cm by controlling the immersion depth of the diffuser in the solution. The bursting bubble aerosol was collected using a glass slide fixed above the liquid surface, as described in our earlier publication.[32] Typically, ca. 50 μL of aerosol was collected within 5 min at the bubbling flow rate of 2 mL/min. The molar concentration of rhodamines in the collected aerosol was measured by UV−vis absorption spectroscopy (2J1-0004 U-2900UV/VIS Dual beam spectrophotometer, Hitachi, Japan). Every experiment, including the preparation of stock solutions, aerosol collection, and UV−vis detection, was repeated in five technical replicates. For each rhodamine solution, E-values were determined as a function of C_{bulk} and bubble path (h) (Figures 1−4). Every bar in the graphs corresponds to the average of at least five independent experiments repeated using freshly prepared solutions. The experimental results were analyzed in reference to the data on rhodamine adsorption at the stationary plane water−air interface and earlier studies of the bubble bursting.[51]

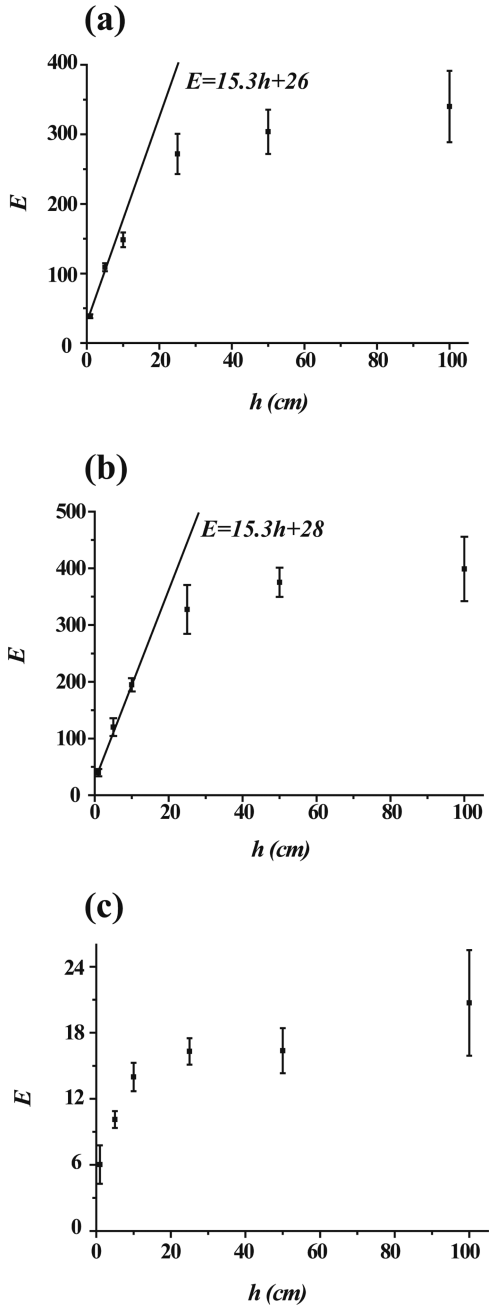

Figure 1. Dependence of surfactant enrichment in bursting bubble aerosol, relative to the bulk solution ($E = C_{aer}/C_{bulk}$), on bubble path (h) from individual 10^{-6} M aqueous solutions of R101 (a), RB (b), and R6G (c). No clear linear slope was revealed for R6G.

RESULTS AND DISCUSSION

Bubble Bursting at the Solution Surface. It is convenient to start the description of surfactant enrichment in bursting bubble aerosol by considering the process of the bubble bursting. There are two principal mechanisms whereby a bubble that has reached the solution surface can burst: film droplet formation and jet droplet formation.[52] It has been experimentally demonstrated in earlier studies that individual gas bubbles in aqueous solutions with a diameter <2 mm produce mostly jet droplets upon bursting, although the presence of film drops cannot be fully eliminated.[14,52] The average diameter of bubbles reaching the surface in our experiments was ca. 0.5 mm, and, therefore, it can be

DOI: 10.1021/acsomega.8b01157
ACS Omega 2018, 3, 8709−8717

concluded that the chemical transfer was mainly contributed by jet droplets. While film droplets are formed upon the collapse of the upper liquid film of the bubble,[53] jet droplets are rather formed from the bottom of the bubble.[19,54] In the jet droplet mechanism, the top film separating the bubble from the atmosphere drains back to solution by gravitational forces. The produced sub-millimeter-sized cavity is subjected to the restoring force, which tends to flatten this cavity by capillary forces. These forces give rise to the high-speed vertical jet shooting out above the free surface. The jet then breaks into a train of 1−10 droplets.[17,54]

The jet droplet mechanism of aerosol formation together with the pronounced dependence of surfactant enrichment in bursting bubble aerosol on bubble path (Figures 1 and 2) strongly indicates that the surfactant molecules mostly make it into the aerosol droplets directly from the surface of individually bursting bubbles rather than from the solution surface or the subsurface microlayer (Figure 5). Hence, it is an important conclusion that the experimentally measured surfactant concentration in the aerosol, C_{aer}, is mainly contributed by surfactant molecules adsorbed from the bulk solution to the surface of rising bubbles, as illustrated in Figure 5. It should also be noted that earlier studies demonstrated that surfactants adsorbed to the bubble surface do not notably affect the characteristics of bubble bursting process as long as they do not induce significant alterations in surface tension.[17] Therefore, for the concentration range studied in our experiments (10^{-4}−10^{-8} M), it is reasonable to assume that C_{aer} should be proportional to the magnitude of surfactant adsorption at the bubble surface, Γ_{bub}, right before bursting.

The contribution of surface solution layer to the overall surfactant concentration in the jet droplet aerosol, C_{aer}, can be roughly estimated by approximating experimental values of surfactant enrichment to the zero-bubble path (h = 0). For example, for R101, $E(h = 0) \approx 26$ and $E(h = 100\ \text{cm}) \approx 350$ (Figure 1a). This means that at h = 100 cm, the contribution of surface solution layer to the overall C_{aer} can be estimated equal to ca. 7%, and the rest, ca. 93% of R101 molecules in the aerosol, is accumulated at the surface of a bubble over its rise in solution and is directly released upon bursting. Similar estimation is obtained for RB (Figure 1b). For R6G, the approximation to h = 0 is less accurate because the linear slope is very abrupt (as discussed in detail below) but similar proportionality can be seen (Figure 1c). Our estimations for R101, RB, and R6G well agree with the earlier reports that the carbon enrichment in the ocean surface microlayer are generally small (<10) compared to those in ocean aerosols (>100), suggesting that contributions from the microlayer probably account for relatively minor fractions of the released carbon under most conditions.[24,27,42] Of course, the collective bubble effects at the surface (such as foaming in breaking waves) should introduce additional complications to the behavior of individual bubbles, e.g., due to the onset of film bursting mechanism.[22,30,44−46] It may be expected that the onset of film bursting mechanism should enhance the release of surfactants adsorbed at the solution surface. The impact of collective effects at the solution surface on the chemical concentration enrichment by bubble bursting is the subject for further research.

Bubble Rise in Bulk Solution. Given the proportionality between C_{aer} and Γ_{bub} right before bursting, we can use the magnitude of C_{aer} and its dependence on h and C_{bulk} to characterize the dynamics of surfactant adsorption on a rising bubble in solution. According to the current mechanistic description, a gas bubble rising from the bottom of a bulk solution adsorbs surface-active solutes and carry them toward the solution surface.[52] Our results demonstrate that during its rise to the solution surface, a bubble passes three successive ranges of molecular adsorption with strongly distinct characteristics: (a) linear kinetic adsorption; (b) mixed kinetic adsorption; and (c) equilibrium adsorption (Figure 5).

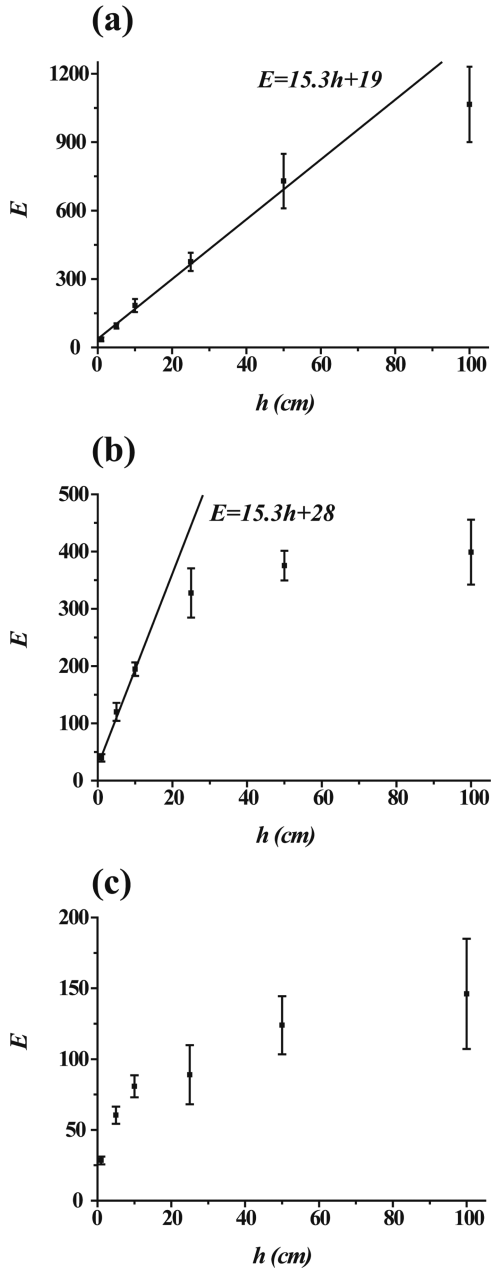

Figure 2. Dependence of surfactant enrichment in bursting bubble aerosol, relative to bulk solution ($E = C_{aer}/C_{bulk}$), on bubble path (h) for RB at $C_{bulk} = 10^{-7}$ M (a), $C_{bulk} = 10^{-6}$ M (b), *and* $C_{bulk} = 10^{-5}$ M (c). No clear linear slope was revealed at 10^{-5} M.

Linear Kinetic Adsorption. The linear kinetic regime of adsorption corresponds to the earliest stage of bubble rise, when Γ_{bub} is still too low to cause any notable activation energy barrier of adsorption or molecular desorption back from the interface. Due to the lack of activation energy barrier, the linear kinetic regime of molecular adsorption to bubble can be

DOI: 10.1021/acsomega.8b01157
ACS Omega 2018, 3, 8709−8717

viewed somewhat analogous to the diffusion-controlled dynamic adsorption in classical models of stationary interfaces.[55] However, contrary to the diffusion-controlled adsorption at the stationary interface, the fluid surrounding the bubble is constantly renewed due to the bubble movement. As a result, the rate of purely linear kinetic adsorption is determined by the rate at which a rising bubble runs upon surfactant solutes rather than by molecular diffusion. In the linear kinetic mode, every surfactant molecule that is run upon by a rising bubble gets adsorbed.

Here, we use a simple model to estimate the molecular adsorption in the linear kinetic mode. Upon its rise in solution over the path h, a bubble of diameter d_{bub} sweeps the volume equal to $(\pi {d_{bub}}^2/4) \times h$. This volume contains $(\pi {d_{bub}}^2/4) \times h \times C_{bulk}$ moles of surfactant. On the basis of the premise that every surfactant molecule in this volume gets adsorbed, the magnitude of Γ_{bub} is increased by $(\pi {d_{bub}}^2/4) \times h \times C_{bulk}/(\pi {d_{bub}}^2) = h \times C_{bulk}/4$. In other words, in the linear kinetic mode

$$(\partial \Gamma_{bub}/\partial h)_T = C_{bulk}/4 \quad (1)$$

To translate the estimate for Γ_{bub} into the domain of experimentally measured C_{aer} and E, we evaluated the total amount of surfactant and solution volume released upon single bubble bursting. For the bubble size range relevant to our study (diameter, 0.2−1.8 mm), Kientzler et al.,[19] using the direct photographic approach, measured the size of the produced jet droplets to be on the order of one-tenth of the bubble size, each bubble producing about five droplets. Therefore, upon bursting one bubble, the total volume of released droplets ($\sum v_{drop}$) is equal to $\sim 0.1^3 \times 5 = 0.005$ of its own volume (v_{bub}). The average diameter of rising bubbles (d_{bub}) in our experiments was ca. 0.5 mm and was not visibly changed with h. Therefore, the net amount of surfactant molecules (in moles) released into aerosol upon bursting of one bubble can be estimated as $\sum \mu_{drop} \sim 0.005 \times C_{aer} \times v_{bub} = 0.005 \times E \times C_{bulk} \times v_{bub}$. As discussed above, the major share of surfactant molecules in the bursting bubble aerosol arrives from the bubble surface. In other words, $\mu_{bub} \approx \sum \mu_{drop}$. Surfactant adsorption at the bubble surface is derived as

$$\Gamma_{bub} = \mu_{bub}/s_{bub} \approx 0.005 \times E \times C_{bulk} \times v_{bub}/s_{bub} = 0.00083 \times E \times C_{bulk} \times d_{bub} \quad (2)$$

From eq 1 and eq 2, we can predict the dependence of E on h in linear kinetic adsorption: $(\partial E/\partial h)_T \approx 300/d_{bub}$. At $d_{bub} \approx 0.5$ mm, our model predicts $(\partial E/\partial h)_T \approx 15$ cm^{-1}. This means that in the linear kinetic range, the magnitude of C_{aer} should increase by ca. $15 \times C_{bulk}$ over every centimeter of bubble rise. Furthermore, our predictions indicate that the magnitude of the linear slope $(\partial E/\partial h)_T$ should be largely independent of C_{bulk} and of surfactant properties. The major parameter responsible for the magnitude of linear slope $(\partial E/\partial h)_T$ is the bubble size. The smaller the bubble diameter, the larger is the slope. This behavior was experimentally observed in earlier studies.[24,32]

The predicted behaviors are in very good qualitative and quantitative agreement with experiments (Figures 1 and 2), which yield a strong support for the relevance of our model. Thus, the magnitude of the linear slope in our experiments is measured as $(\partial E/\partial h)_T \approx 15.3$ cm^{-1} for RB and R101 at 10^{-7} and 10^{-6} M (Figures 1a,b and 2a,b). This is the maximal possible rate of enrichment for any surfactant under the bubbling conditions used in our study. It should be noted that the span of the kinetic range shrinks with C_{bulk} due to the faster saturation of the bubble surface. For RB, the span of the linear range was $h \sim 50$ cm (which corresponds to ∼2.5 s of rise time) at $C_{bulk} = 10^{-7}$ M (Figure 2a), $h \sim 10$ cm at $C_{bulk} = 10^{-6}$ M (Figure 2b) and could not be experimentally identified at $C_{bulk} = 10^{-5}$ M (Figure 2c). Also, the span of the linear kinetic range (but not the rate of adsorption in the linear kinetic range) strongly depends on surfactant properties. The earlier the onset of activation energy barrier of surfactant adsorption, the shorter is the linear kinetic range. Thus, no clear linear kinetic regime could be distinguished for R6G at $C_{bulk} = 10^{-6}$ M (Figure 1c), most probably because R6G displays the particularly early onset of activation energy barrier with C_{bulk}.[51] Our data indicate that R6G displays notably long-ranged linear kinetic adsorption only at $C_{bulk} < 10^{-9}$ M. Thus, at $h = 100$ cm and $C_{bulk} = 10^{-10}$ M, the E-value for R6G becomes nearly equal to the value $E \approx 1550$, predicted by the linear kinetic adsorption equation $(\partial E/\partial h)_T \approx 15.3$ cm^{-1} (Figure 4), which indicates that the adsorption of R6G under those conditions follows linear kinetic mode at least up to the bubble path of 100 cm.

Due to the good agreement between experimental data and the proposed model, we believe that in the linear kinetic mode, surfactant diffusion does not have a notable contribution to the rate of molecular adsorption at the moving bubble surface. Here, we also attempted to apply a model earlier proposed by Ybert and di Meglio[56] to estimate the surfactant flux to the interface of a rising bubble. In their calculations, the authors assumed that the adsorption occurs through diffusion, the role of convection being in a constant renewal of the fluid surrounding the bubble.[56] However, the obtained prediction for adsorption slope $(\partial E/\partial h)_T \approx 72$ cm^{-1} was ca. 5 times higher than the value $(\partial E/\partial h)_T \approx 15.3$ cm^{-1}, as measured in our experiments. Thus, we conclude that under the experimental conditions employed in this study, the linear kinetic adsorption is not controlled by molecular diffusion but rather mainly by bubble movement (convection).

Mixed Kinetic Adsorption. At a certain point (still below equilibrium), further growth of Γ_{bub} (and C_{aer}) with h starts to deviate from linearity and gradually slows down compared to the linear kinetic range (Figures 1 and 2), indicating the onset of mixed kinetic adsorption. The term "mixed kinetic adsorption" is adapted from the classical model of dynamic molecular adsorption at stationary interfaces.[47,48] This term indicates that adsorption is simultaneously driven both by kinetic and thermodynamic factors. There are two principal factors responsible for the slow down in the growth of Γ_{bub} with h in the mixed kinetic range relative to the linear kinetic range. These two factors are the molecular desorption from the bubble and the onset of adsorption activation barrier imposed by the adsorbed surfactant molecules.[55] Molecular desorption slows down the growth of Γ_{bub} with h by enhancing the molecular outflow from the bubble surface, whereas the onset of adsorption activation barrier reduces the molecular inflow onto the bubble surface. Which of these two factors is primarily responsible for the nonlinearity depends upon the properties and concentration of a specific surfactant. For example, in the case of weak molecular adsorption and extremely low C_{bulk}, the concentration of adsorbed surfactant molecules is too low to bring about activation energy barrier of adsorption, and the nonlinearity between Γ_{bub} and h ultimately occurs entirely due to the gradual enhancement of molecular desorption.

DOI: 10.1021/acsomega.8b01157
ACS Omega 2018, 3, 8709−8717

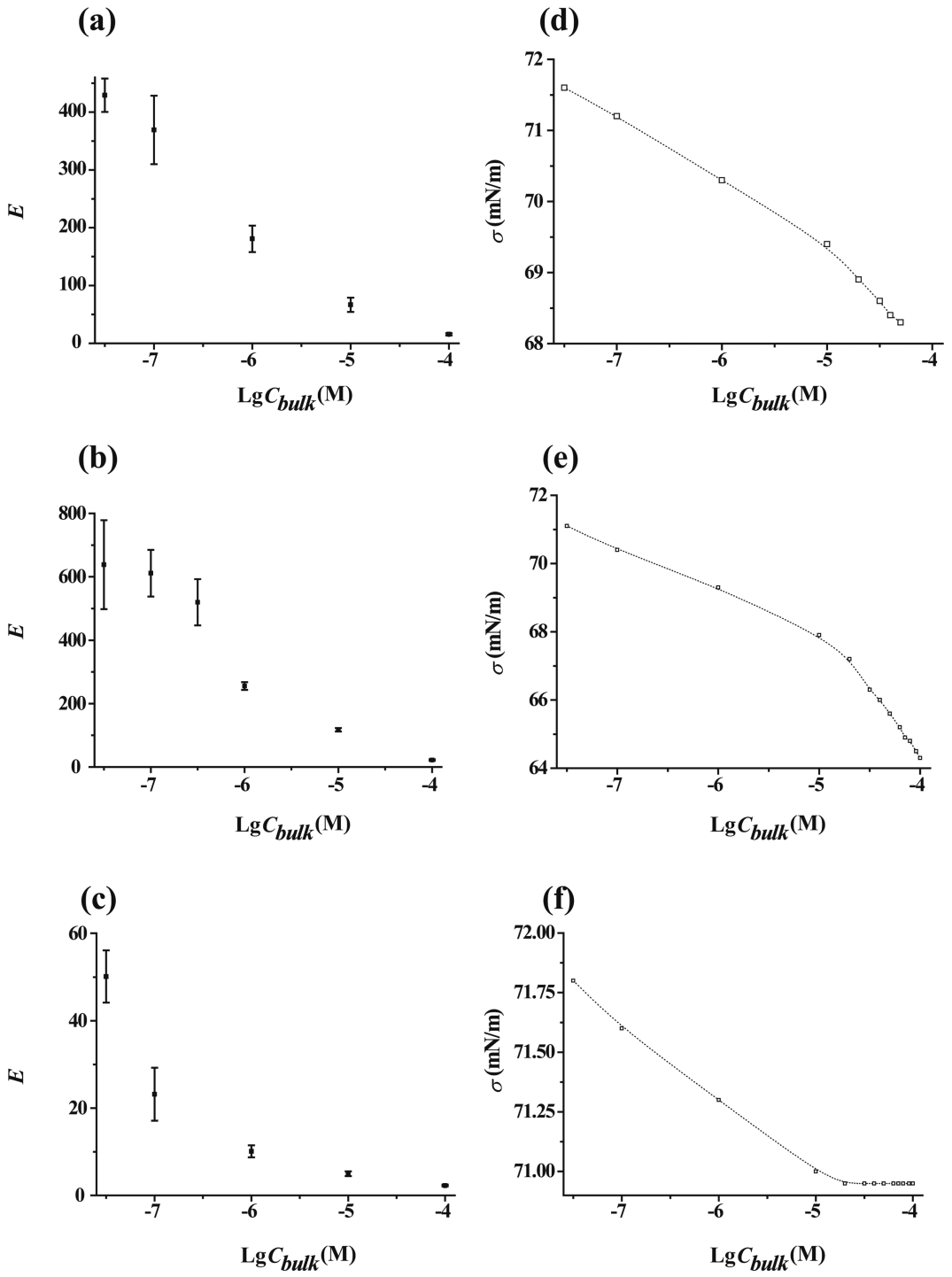

Figure 3. Dependence of surfactant enrichment in bursting bubble aerosol, relative to the bulk solution ($E = C_{aer}/C_{bulk}$), on surfactant concentration in bulk solution (C_{bulk}) from the individual aqueous solutions of R101 (a), RB (b), and R6G (c) at h = 35 cm. The dependence of equilibrium surface tension (σ) on C_{bulk} for the individual aqueous solutions of R101 (d), RB (e), and R6G (f) from ref 51 is shown for reference.

Alternatively, in the case of very strong adsorption, the nonlinearity between Γ_{bub} and h mainly occurs due to the onset of activation energy barrier at the bubble surface. This scenario is commonly relevant to ionic surfactants, such as rhodamines, for which energy tension effects due to electrostatic repulsion at the surface start at very low concentrations.[47,57] Among the three studied rhodamine surfactants, R6G displays particularly rapid elevation in the activation energy barrier of adsorption with C_{bulk},[51] and this is the most likely reason why at equal C_{bulk} the onset of nonlinearity between E and h occurs for R6G much earlier than for RB and for R101 (Figure 1c). Our results indicate the pronounced activation energy barrier of adsorption for R6G, even at $C_{bulk} < 10^{-8}$ M (Figures 3c and 4). The adsorption of R6G becomes nearly linear kinetic at $C_{bulk} \leq 10^{-10}$ M, as indicated by the close similarity between the experimental magnitude of E at $C_{bulk} = 10^{-10}$ M with the magnitude $E \approx 1550$ predicted by the linear kinetic adsorption equation $(\partial E/\partial h)_T \approx 15.3$ cm^{-1} (Figure 4).

Equilibrium Adsorption. In the equilibrium range, the magnitude of surfactant adsorption at the surface of a rising

DOI: 10.1021/acsomega.8b01157
ACS Omega 2018, 3, 8709−8717

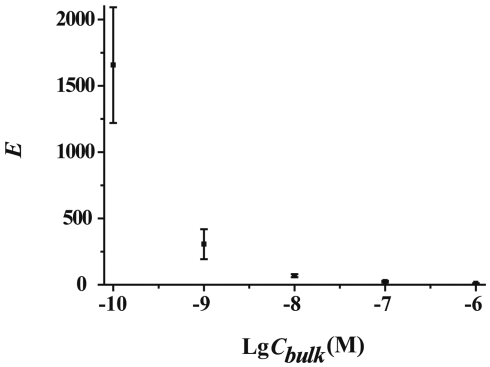

Figure 4. Dependence of R6G enrichment in bursting bubble aerosol, relative to the bulk solution ($E = C_{aer}/C_{bulk}$), on surfactant concentration in bulk solution (C_{bulk}) from the individual aqueous solutions of R6G at h = 100 cm.

bubble, Γ_{bub}, no longer grows with h because the rate of molecular desorption has become equal to the rate of molecular adsorption. The bubble path, over which the equilibrium at a rising bubble surface is attained, largely depends upon C_{bulk}. The higher the C_{bulk}, the more intense is the molecular exchange between the bubble surface interface and bulk solution and, hence, is the faster attainment of equilibrium. In our experiments, the attainment of molecular equilibrium at the bubble surface in RB solutions roughly required $h \sim 15$ cm at $C_{bulk} = 10^{-5}$ M, whereas $h \sim 30$ cm at $C_{bulk} = 10^{-6}$ M. The equilibrium was not reached at $C_{bulk} = 10^{-7}$ M, up to a maximal bubble path h = 100 cm (Figure 2a).

In the ideal scenario, when the turbulence effects, bubble coalescence, and other effects associated with bubble movement do not significantly influence the adsorption process, the equilibrium Γ_{bub} ultimately reached at high bubble paths should be equal to the magnitude of equilibrium adsorption at the stationary water−air interface of aqueous solution (Γ_{sol}) for the same C_{bulk} (Figure 5). For surfactant concentrations well below the critical micelle concentration, the magnitude of equilibrium surfactant adsorption at the interface may be estimated from its surface activity, i.e., the slope of a σ−ln(C_{bulk}) dependence (Figure 3c−e), based on the Gibbs adsorption equation with the ideal dilute solution assumption.[47] For the room-temperature aqueous solutions, at $C_{bulk} = 10^{-5}$ M, the estimated magnitude of equilibrium adsorption at the interface increases the order Γ_{sol}(R6G) ∼ 0.05 μmol/m^2 < Γ_{sol}(R101) ∼ 0.13 < Γ_{sol}(RB) ∼ 0.2 μmol/m^2.[51] Consistently, the magnitude of surfactant enrichment in the bursting bubble aerosol at $C_{bulk} = 10^{-5}$ M and h = 35 cm increases in the same order: E(R6G) ∼ 5 < E(R101) ∼ 65 < E(RB) ∼ 115 (Figure 3). It should be noted that our data indicate that at $C_{bulk} = 10^{-5}$ M and h = 35 cm, the adsorption of rhodamines at the bubble surface definitely reaches equilibrium before bursting (Figure 2). Therefore, the magnitude of surfactant enrichment in the bursting bubble aerosol, produced under the conditions of equilibrium adsorption at the bubble surface, is largely determined by the thermodynamic properties of a surfactant, such as its surface activity.

It should be noted that the surface activity of a surfactant determines the magnitudes of its Γ_{bub} and E, only in the equilibrium adsorption range. In contrast, as we have shown above, in the linear kinetic region, the magnitudes of Γ_{bub} and E are largely independent of the surfactant properties (Figures 1a,b and 2a,b). Thereby, we reveal that the magnitude of

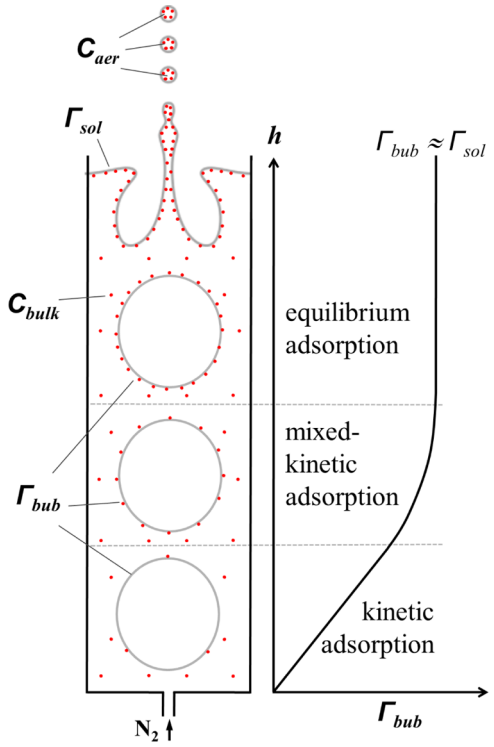

Figure 5. Mechanistic representation for the multistage surfactant adsorption at the surface of rising gas bubbles and surfactant enrichment in the aerosols produced by individually bursting bubbles.

surfactant enrichment in bursting bubble aerosols strongly depends upon which mode of adsorption (kinetic, mixed kinetic, or equilibrium) is in control by the moment of the bubble bursting for the particular surfactant (Figure 5).

Estimation of Equilibrium Adsorption at the Bubble Surface. We use the experimental magnitudes of surfactant concentration in bursting bubble aerosols, C_{aer}, obtained in the equilibrium adsorption range to evaluate the equilibrium Γ_{bub} right before bursting. Using eq 2 and the experimental values from Figure 3, at $C_{bulk} = 10^{-5}$ M, we calculate Γ_{bub}(RB) ∼ 0.4 μmol/m^2, Γ_{bub}(R101) ∼ 0.3 μmol/m^2, and Γ_{bub}(R6G) ∼ 0.02 μmol/m^2. These very rough estimates for Γ_{bub} are surprisingly in good agreement with the earlier estimated adsorption of rhodamines at the stationary air−water interface, Γ_{sol}, derived from the surface tension measurements at the same C_{bulk}: Γ_{sol}(RB) ∼ 0.2 μmol/m^2, Γ_{sol}(R101) ∼ 0.13 μmol/m^2, and Γ_{sol}(R6G) ∼ 0.05 μmol/m^2.[51] The close similarity between the magnitudes of Γ_{bub} in the equilibrium region estimated based on C_{aer} and the magnitudes of Γ_{sol} indicates that the adsorption process to the bubble surface in equilibrium range is well described using the models developed for stationary interfaces.

Surfactant Enrichment in Bursting Bubbles vs Molecular Concentration. Our data indicate that at $C_{bulk} \geq 10^{-6}$ M and $h \geq 35$ cm, the magnitude of Γ_{bub} for R6G, R101, and RB reaches the equilibrium level before bursting (Figures 1 and 2). Therefore, the experimental values of E for bursting bubble aerosols can be discussed in direct relation to the data on equilibrium surface tension at the stationary water−air surface interface (σ). Under equilibrium conditions ($C_{bulk} \geq 10^{-6}$ M), both σ and E decrease with C_{bulk} (Figure 3), but the causes are different. The decrease of σ with C_{bulk} is directly caused by the growing number of surface- active molecules at the interface, whereas the decrease of E with C_{bulk}

DOI: 10.1021/acsomega.8b01157
ACS Omega 2018, 3, 8709−8717

is rather caused by the increase of activation energy barrier in adsorption associated with the growing number of surface-active molecules at the interface.[47,57,58] In simple words, fewer and fewer new surfactant molecules attach to the bubble surface, as the magnitude of C_{bulk} is increased. At a certain C_{bulk}, the surface becomes fully saturated, i.e., a further increase in C_{bulk} brings no new molecules to the surface. As a result, σ levels off to a certain value. It should be noted that the magnitude $E = C_{aer}/C_{bulk}$ continues to decrease with C_{bulk} even after surface saturation (Figure 3). For the same surfactant, the magnitude of E can span 3 orders of magnitude depending on C_{bulk} (Figures 3 and 4). Therefore, apart from the surface activity, the surfactant concentration in bulk solution is another important factor that determines the magnitude of surfactant enrichment in bursting bubble aerosols in the equilibrium adsorption region.

At very low C_{bulk}, the surfactant adsorption does not reach equilibrium before bubble bursting and rather follows the linear kinetic regime. At h = 35 cm, the linear kinetic adsorption equation $(\partial E/\partial h)_T \approx 15.3\ cm^{-1}$ predicts the magnitude $E \approx 560$ for all surfactants. This predicted value is experimentally reached for RB (Figure 3b) and nearly reached for R101 (Figure 3a) at $C_{bulk} \leq 10^{-7}$ M, indicating that the adsorption of these surfactants up to the moment of bubble bursting mainly follows linear or near-linear kinetics. In contrast, the E-value of R6G is much lower than the predicted value for linear kinetic adsorption, which suggests a substantial role of the activation energy barrier (Figure 3c). Our data suggest that the linear kinetic range for R6G is only reached at $C_{bulk} \leq 10^{-10}$ M, at which point the measured E-value is roughly equal to the value predicted by the linear kinetic adsorption equation (Figure 4).

SUMMARY AND CONCLUSIONS

Our results allow a comprehensive quantitative description for the enrichment behavior of surface-active compounds in the aerosols produced by individually bursting bubbles. The process of chemical transfer by bubble bursting is illustrated in Figure 5. A bubble rising in the solution successively passes three distinct ranges of surfactant adsorption: linear kinetic, mixed kinetic, and equilibrium. In linear kinetic range, the rate of adsorption is largely independent of surfactant properties and is mainly determined by the surfactant concentration in solution and bubble size. The span of the linear kinetic range strongly depends on the surfactant properties and may extend beyond the bubble paths of several meters. In equilibrium range, the adsorption of surfactants solutes to the bubble surface is well described using the terms of equilibrium models for stationary interfaces, and the enrichment of surfactant solutes depends upon their surface activity and bulk surfactant concentration. At the solution surface, the bubble breaks up into jet droplets. Our data indicate that surfactant molecules are mainly transferred into the droplets upon bubble bursting directly from the surface of the bursting bubble rather than from the solution surface or from the immediate surface layer of bulk solution. This conclusion is consistent with the fact that the jet droplets are mainly formed from the bottom interfacial layers of the bubble, whereas the top interfacial layers are rather drained back to the bulk solution (Figure 5). Our results thereby provide a step-by-step description of the chemical transfer by the bursting of individual bubbles at a calm solution surface. This description consistently resolves a great deal of uncertainty regarding the variability of experimental behaviors. Thus, it shows that variability in the relative partitioning of surfactant solutes to the aerosol phase is related to which mode of adsorption is at operation for each particular surfactant under given bubbling conditions. While the experimental conditions in the current study were chosen for the simplicity of mechanistic consideration, further research will address the complications to this basic description due to the collective effects at the surface, including bubble coalescence, foaming, ripples, etc., which commonly accompany bubble bursting in sea spray aerosols as well as in other natural environments.

AUTHOR INFORMATION

Corresponding Author

*E-mail: chw8868@gmail.com. Fax: (+86)791-83896370.

ORCID

Konstantin Chingin: 0000-0003-4670-8859

Author Contributions

R.Y. and D.Z. performed the experiments; R.Y., D.Z., and K.C. analyzed the data; K.C. and H.C. conceived the idea of the project and wrote the manuscript.

Notes

The authors declare no competing financial interest.

ACKNOWLEDGMENTS

The research was supported by the National Natural Science Foundation of China (nos. 21520102007, 21305012), Program for Changjiang Scholars and Innovative Research Team in Universities (PCSIRT) (no. IRT_17R20), and 111 Project (no. D17006).

REFERENCES

(1) Woodcock, A. H.; Kientzler, C. F.; Arons, A. B.; Blanchard, D. C. Giant Condensation Nuclei from Bursting Bubbles. *Nature* **1953**, *172*, 1144.

(2) Bird, J. C.; de Ruiter, R.; Courbin, L.; Stone, H. A. Daughter bubble cascades produced by folding of ruptured thin films. *Nature* **2010**, *465*, 759.

(3) Blanchard, D. C. Electrified Droplets from the Bursting of Bubbles at an Air−Sea Water Interface. *Nature* **1955**, *175*, 334.

(4) Mason, B. J. Bursting of Air Bubbles at the Surface of Sea Water. *Nature* **1954**, *174*, 470−471.

(5) Blanchard, D. C.; Syzdek, L. Mechanism for the Water-to-Air Transfer and Concentration of Bacteria. *Science* **1970**, *170*, 626−628.

(6) Baylor, E. R.; Baylor, M. B.; Blanchard, D. C.; Syzdek, L. D.; Appel, C. Virus Transfer from Surf to Wind. *Science* **1977**, *198*, 575−580.

(7) Gantt, B.; Meskhidze, N. The physical and chemical characteristics of marine primary organic aerosol: a review. *Atmos. Chem. Phys.* **2013**, *13*, 3979−3996.

(8) Russell, L. M.; Hawkins, L. N.; Frossard, A. A.; Quinn, P. K.; Bates, T. S. Carbohydrate-like composition of submicron atmospheric particles and their production from ocean bubble bursting. *Proc. Natl. Acad. Sci. U.S.A.* **2010**, *107*, 6652−6657.

(9) Veron, F. Ocean Spray. In *Annual Review of Fluid Mechanics*; Davis, S. H.; Moin, P., Eds.; Annual Reviews: Palo Alto, 2015; Vol. *47*, pp 507−538.

(10) Cochran, R. E.; Ryder, O. S.; Grassian, V. H.; Prather, K. A. Sea Spray Aerosol: The Chemical Link between the Oceans, Atmosphere, and Climate. *Acc. Chem. Res.* **2017**, *50*, 599−604.

(11) Quinn, P. K.; Collins, D. B.; Grassian, V. H.; Prather, K. A.; Bates, T. S. Chemistry and Related Properties of Freshly Emitted Sea Spray Aerosol. *Chem. Rev.* **2015**, *115*, 4383−4399.

(12) de Leeuw, G.; Andreas, E. L.; Anguelova, M. D.; Fairall, C. W.; Lewis, E. R.; O'Dowd, C.; Schulz, M.; Schwartz, S. E. Production flux of sea spray aerosol. *Rev. Geophys.* **2011**, *49*, No. RG2001.

DOI: 10.1021/acsomega.8b01157
ACS Omega 2018, 3, 8709−8717

(13) Liger-Belair, G.; Cilindre, C.; Gougeon, R. D.; Lucio, M.; Gebefugi, I.; Jeandet, P.; Schmitt-Kopplin, P. Unraveling different chemical fingerprints between a champagne wine and its aerosols. *Proc. Natl. Acad. Sci. U.S.A.* **2009**, *106*, 16545−16549.
(14) Liger-Belair, G.; Lemaresquier, H.; Robillard, B.; Duteurtre, B.; Jeandet, P. The Secrets of Fizz in Champagne Wines: A Phenomenological Study. *Am. J. Enol. Vitic.* **2001**, *52*, 88−92.
(15) Péron, N.; Cagna, A.; Valade, M.; Bliard, C.; Aguié-Béghin, V.; Douillard, R. Layers of Macromolecules at the Champagne/Air Interface and the Stability of Champagne Bubbles. *Langmuir* **2001**, *17*, 791−797.
(16) Peron, N.; Meunier, J.; Cagna, A.; Valade, M.; Douillard, R. Phase separation in molecular layers of macromolecules at the champagne-air interface. *J. Microsc.* **2004**, *214*, 89−98.
(17) Séon, T.; Liger-Belair, G. Effervescence in champagne and sparkling wines: From bubble bursting to droplet evaporation. *Eur. Phys. J.: Spec. Top.* **2017**, *226*, 117−156.
(18) Liger-Belair, G.; Marchal, R.; Robillard, B.; Dambrouck, T.; Maujean, A.; Vignes-Adler, M.; Jeandet, P. On the Velocity of Expanding Spherical Gas Bubbles Rising in Line in Supersaturated Hydroalcoholic Solutions: Application to Bubble Trains in Carbonated Beverages. *Langmuir* **2000**, *16*, 1889−1895.
(19) Kientzler, C. F.; Arons, A. B.; Blanchard, D. C.; Woodcock, A. H. Photographic Investigation of the Projection of Droplets by Bubbles Bursting at a Water Surface1. *Tellus* **1954**, *6*, 1−7.
(20) Ke, W.-R.; Kuo, Y.-M.; Lin, C.-W.; Huang, S.-H.; Chen, C.-C. Characterization of aerosol emissions from single bubble bursting. *J. Aerosol Sci.* **2017**, *109*, 1−12.
(21) Tran, T. T.; Lee, E. G.; Lee, I. S.; Woo, N. S.; Han, S. M.; Kim, Y. J.; Hwang, W. R. Hydrodynamic extensional stress during the bubble bursting process for bioreactor system design. *Korea Aust. Rheol. J.* **2016**, *28*, 315−326.
(22) Lee, J. S.; Weon, B. M.; Park, S. J.; Je, J. H.; Fezzaa, K.; Lee, W.-K. Size limits the formation of liquid jets during bubble bursting. *Nat. Commun.* **2011**, *2*, No. 367.
(23) Prather, K. A.; Bertram, T. H.; Grassian, V. H.; Deane, G. B.; Stokes, M. D.; DeMott, P. J.; Aluwihare, L. I.; Palenik, B. P.; Azam, F.; Seinfeld, J. H.; Moffet, R. C.; Molina, M. J.; Cappa, C. D.; Geiger, F. M.; Roberts, G. C.; Russell, L. M.; Ault, A. P.; Baltrusaitis, J.; Collins, D. B.; Corrigan, C. E.; Cuadra-Rodriguez, L. A.; Ebben, C. J.; Forestieri, S. D.; Guasco, T. L.; Hersey, S. P.; Kim, M. J.; Lambert, W. F.; Modini, R. L.; Mui, W.; Pedler, B. E.; Ruppel, M. J.; Ryder, O. S.; Schoepp, N. G.; Sullivan, R. C.; Zhao, D. Bringing the ocean into the laboratory to probe the chemical complexity of sea spray aerosol. *Proc. Natl. Acad. Sci. U.S.A.* **2013**, *110*, 7550−7555.
(24) Tseng, R.-S.; Viechnicki, J. T.; Skop, R. A.; Brown, J. W. Sea-to-air transfer of surface-active organic compounds by bursting bubbles. *J. Geophys. Res.: Oceans* **1992**, *97*, 5201−5206.
(25) Collins, D. B.; Zhao, D. F.; Ruppel, M. J.; Laskina, O.; Grandquist, J. R.; Modini, R. L.; Stokes, M. D.; Russell, L. M.; Bertram, T. H.; Grassian, V. H.; Deane, G. B.; Prather, K. A. Direct aerosol chemical composition measurements to evaluate the physicochemical differences between controlled sea spray aerosol generation schemes. *Atmos. Meas. Tech.* **2014**, *7*, 3667−3683.
(26) Schmitt-Kopplin, P.; Liger-Belair, G.; Koch, B. P.; Flerus, R.; Kattner, G.; Harir, M.; Kanawati, B.; Lucio, M.; Tziotis, D.; Hertkorn, N.; Gebefugi, I. Dissolved organic matter in sea spray: a transfer study from marine surface water to aerosols. *Biogeosciences* **2012**, *9*, 1571−1582.
(27) Keene, W. C.; Maring, H.; Maben, J. R.; Kieber, D. J.; Pszenny, A. A. P.; Dahl, E. E.; Izaguirre, M. A.; Davis, A. J.; Long, M. S.; Zhou, X.; Smoydzin, L.; Sander, R. Chemical and physical characteristics of nascent aerosols produced by bursting bubbles at a model air-sea interface. *J. Geophys. Res.: Atmos.* **2007**, *112*, No. D21202.
(28) O'Dowd, C. D.; Facchini, M. C.; Cavalli, F.; Ceburnis, D.; Mircea, M.; Decesari, S.; Fuzzi, S.; Yoon, Y. J.; Putaud, J. P. Biogenically driven organic contribution to marine aerosol. *Nature* **2004**, *431*, 676−80.
(29) McNeill, V. F.; Sareen, N.; Schwier, A. N. Surface-Active Organics in Atmospheric Aerosols. In *Atmospheric and Aerosol Chemistry*; McNeill, V. F.; Ariya, P. A., Eds.; 2014; Vol. *339*, pp 201−259.
(30) Cochran, R. E.; Jayarathne, T.; Stone, E. A.; Grassian, V. H. Selectivity Across the Interface: A Test of Surface Activity in the Composition of Organic-Enriched Aerosols from Bubble Bursting. *J. Phys. Chem. Lett.* **2016**, *7*, 1692−1696.
(31) Chingin, K.; Cai, Y.; Chagovets, V.; Kononikhin, A.; Starodubtseva, N.; Frankevich, V.; Chen, H. Preconcentration of organic solutes in urine by bubble bursting. *Metabolomics* **2016**, *12*, 171.
(32) Chingin, K.; Cai, Y.; Liang, J.; Chen, H. Simultaneous Preconcentration and Desalting of Organic Solutes in Aqueous Solutions by Bubble Bursting. *Anal. Chem.* **2016**, *88*, 5033−5036.
(33) Deane, G. B.; Stokes, M. D. Scale dependence of bubble creation mechanisms in breaking waves. *Nature* **2002**, *418*, 839.
(34) Stokes, M. D.; Deane, G. B.; Prather, K.; Bertram, T. H.; Ruppel, M. J.; Ryder, O. S.; Brady, J. M.; Zhao, D. A Marine Aerosol Reference Tank system as a breaking wave analogue for the production of foam and sea-spray aerosols. *Atmos. Meas. Tech.* **2013**, *6*, 1085−1094.
(35) Blanchette, F.; Bigioni, T. P. Partial coalescence of drops at liquid interfaces. *Nat. Phys.* **2006**, *2*, 254.
(36) Donaldson, D. J.; Vaida, V. The Influence of Organic Films at the Air−Aqueous Boundary on Atmospheric Processes. *Chem. Rev.* **2006**, *106*, 1445−1461.
(37) Perrine, K. A.; Parry, K. M.; Stern, A. C.; Van Spyk, M. H. C.; Makowski, M. J.; Freites, J. A.; Winter, B.; Tobias, D. J.; Hemminger, J. C. Specific cation effects at aqueous solution−vapor interfaces: Surfactant-like behavior of Li+ revealed by experiments and simulations. *Proc. Natl. Acad. Sci. U.S.A.* **2017**, *114*, 13363−13368.
(38) Kuzmenko, I.; Rapaport, H.; Kjaer, K.; Alsnielsen, J.; Weissbuch, I.; Lahav, M.; Leiserowitz, L. Design and characterization of crystalline thin film architectures at the air-liquid interface: simplicity to complexity. *Chem. Rev.* **2001**, *101*, 1659−1696.
(39) Cochran, R. E.; Laskina, O.; Jayarathne, T.; Laskin, A.; Laskin, J.; Lin, P.; Sultana, C.; Lee, C.; Moore, K. A.; Cappa, C. D.; Bertram, T. H.; Prather, K. A.; Grassian, V. H.; Stone, E. A. Analysis of Organic Anionic Surfactants in Fine and Coarse Fractions of Freshly Emitted Sea Spray Aerosol. *Environ. Sci. Technol.* **2016**, *50*, 2477−2486.
(40) Lewis, E. R.; Schwartz, S. E. *Sea Salt Aerosol Production: Mechanisms, Methods, Measurements and Models*, 1st ed.; American Geophysical Union: Washington, DC, 2004.
(41) Debrégeas, G.; de Gennes, P.-G.; Brochard-Wyart, F. The Life and Death of "Bare" Viscous Bubbles. *Science* **1998**, *279*, 1704−1707.
(42) Hunter, K. A. Chemistry of the Sea-Surface Microlayer. In *The Sea Surface and Global Change*; Liss, P. S.; Duce, R. A., Eds.; Cambridge University Press: New York, 1997; pp 287−319.
(43) Hoffman, E. J.; Duce, R. A. Factors influencing the organic carbon content of marine aerosols: A laboratory study. *J. Geophys. Res.* **1976**, *81*, 3667−3670.
(44) Leck, C.; Bigg, E. K. Source and evolution of the marine aerosol—A new perspective. *Geophys. Res. Lett.* **2005**, *32*, No. L19803.
(45) Bezdek, H. F.; Carlucci, A. F. Concentration and removal of liquid microlayers from a seawater surface by bursting bubbles1. *Limnol. Oceanogr.* **1974**, *19*, 126−132.
(46) Gershey, R. M. Characterization of seawater organic matter carried by bubble-generated aerosols1. *Limnol. Oceanogr.* **1983**, *28*, 309−319.
(47) Chang, C.-H.; Franses, E. I. Adsorption dynamics of surfactants at the air/water interface: a critical review of mathematical models, data, and mechanisms. *Colloids Surf., A* **1995**, *100*, 1−45.
(48) Eastoe, J.; Dalton, J. S. Dynamic surface tension and adsorption mechanisms of surfactants at the air−water interface. *Adv. Colloid Interface Sci.* **2000**, *85*, 103−144.
(49) Vasudevan, D.; Fimmen, R. L.; Francisco, A. B. Tracer-grade rhodamine WT: structure of constituent isomers and their sorption behavior. *Environ. Sci. Technol.* **2001**, *35*, 4089−4096.

DOI: 10.1021/acsomega.8b01157
ACS Omega 2018, 3, 8709−8717

(50) Gao, W.; Wu, N.; Du, J.; Zhou, L.; Lian, Y.; Wang, L.; Liu, D. Occurrence of rhodamine B contamination in capsicum caused by agricultural materials during the vegetation process. *Food Chem.* **2016**, *205*, 106−111.
(51) Seno, K.; Ishioka, T.; Harata, A.; Hatano, Y. Photoionization of Rhodamine Dyes Adsorbed at the Aqueous Solution Surfaces Investigated by Synchrotron Radiation. *Anal. Sci.* **2002**, *17*, i1177−i1179.
(52) Resch, F. J.; Darrozes, J. S.; Afeti, G. M. Marine liquid aerosol production from bursting of air bubbles. *J. Geophys. Res.: Oceans* **1986**, *91*, 1019−1029.
(53) Lhuissier, H.; Villermaux, E. Bursting bubble aerosols. *J. Fluid Mech.* **2012**, *696*, 5−44.
(54) Blanchard, D. C. The electrification of the atmosphere by particles from bubbles in the sea. *Prog. Oceanogr.* **1963**, *1*, 73−202.
(55) Ward, A. F. H.; Tordai, L. Time-Dependence of Boundary Tensions of Solutions I. The Role of Diffusion in Time-Effects. *J. Chem. Phys.* **1946**, *14*, 453−461.
(56) Ybert, C.; di Meglio, J.-M. Ascending air bubbles in protein solutions. *Eur. Phys. J. B* **1998**, *4*, 313−319.
(57) Prosser, A. J.; Franses, E. I. Adsorption and surface tension of ionic surfactants at the air−water interface: review and evaluation of equilibrium models. *Colloids Surf., A* **2001**, *178*, 1−40.
(58) Shchukin, E. D.; Pertsov, A. V.; Amelina, E. A.; Zelenev, A. S. *Colloid and Surface Chemistry*; Elsevier: Amsterdam, 2001; Vol. *12*.

DOI: 10.1021/acsomega.8b01157
ACS Omega 2018, 3, 8709−8717